

# INCREASED INTENSITY PERFORMANCE OF THE BROOKHAVEN AGS\*

E. Raka, L. Ahrens, W. Frey, E. Gill, J.W. Glenn, R. Sanders  
AGS Department, Brookhaven National Laboratory  
Upton, New York 11973

W. Weng  
Stanford Linear Accelerator Center  
Stanford, CA 94305

## Summary

With the advent of  $H^-$  injection into the Brookhaven AGS, circulating beams of up to  $3 \times 10^{13}$  protons at 200 MeV have been obtained. Rf capture of  $2.2 \times 10^{13}$  and acceleration of  $1.73 \times 10^{13}$  up to the transition energy ( $\approx 8$  GeV) and  $1.64 \times 10^{13}$  to full energy ( $\approx 29$  GeV) has been achieved. This represents a 50% increase over the best performance obtained with  $H^+$  injection. The increase in circulation beam current is obtained without filling the horizontal aperture. This allows the rf capture process to utilize a larger longitudinal phase space area ( $\approx 1$  eV sec/bunch vs  $\leq 0.6$  eV sec with  $H^+$  operation). The resulting reduction in relative longitudinal density partially offsets the increase in space charge effects at higher currents. In order to make the capture process independent of injected beam current, a dynamic beam loading compensation loop was installed on the AGS rf system. This is the only addition to the synchrotron itself that was required to reach the new intensity records. A discussion of injection, the rf capture process, and space charge effects is presented.

## Injection

At present it is possible to obtain  $3 \times 10^{13}$  protons circulating in the AGS with  $H^-$  injection.<sup>1</sup> This intensity is achieved with a 300  $\mu$ sec linac beam pulse of  $\approx 20$  mA, representing an injection efficiency of about 75%. Operationally, injection is such that in the horizontal plane the beam comes in to the outside of the  $\lambda/2$  closed orbit bump located at the stripping foil. Since this bump is at present not ramped, the position error increases during the injection pulse. In the vertical plane injection is normally tangential to the closed orbit. Significant dilution of the  $3.5 \pi$  mm-mrad normalized horizontal and vertical linac emittances occur during the injection process. IPM<sup>2</sup> measurements of the spiraling injected beam without rf voltage give rms beam sizes of  $\approx 10$  mm in both planes at a  $\beta = R/Q_{xy} = 15$  M. This corresponds to a 95% emittance of  $25 \pi$  mm-mrad. The off orbit injection mode is certainly responsible for some of the horizontal growth but the vertical growth is not understood.

When the rf voltage is on, the amount of beam remaining in the machine after injection is terminated is  $1-2 \times 10^{12}$  less with typical operational values being  $2.4-2.6 \times 10^{13}$ . The vertical beam size does not change with the capture process while the horizontal emittance grows as described in the next section. Actually, the normalized vertical emittance remains essentially the same during the first 30-50 msec after injection during which all the capture and resonance losses occur. The  $5\sigma$  beam size at a  $\beta_{max}$  is  $\approx 2.8''$  while the nominal aperture is  $3.2''$ . This behavior suggests that at high intensity all the available vertical aperture is filled right at

injection. It should be noted that with the present mode of injection, matching the linac emittance to the AGS lattice is not necessary. Presumably the resulting phase space dilution is required to reduce the effects of space charge.

## Capture and Acceleration

The nominal magnetic field rise rate during injection and early acceleration is 0.49 T/sec. Hence, the central equilibrium orbit energy changes by  $\approx 2.1$  MeV for a 300  $\mu$ sec injected beam, while the linac energy remains constant (linac energy spread  $< 0.8$  MeV). A two-level voltage program is employed in the capture process as can be seen in Fig. 1. During injection, the initial level is  $\approx 150$  kV which produces an rf bucket of 3.2 MeV full width at the synchronous  $f$  of 33 Kc/msec. Then a rise to  $\approx 300$  kV in about 300  $\mu$ sec is added. At this voltage the phase oscillation frequency is 6.6 Kc and the full bucket height is  $\approx 5.3$  MeV.

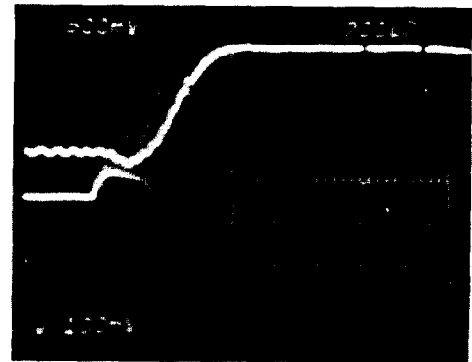


Fig. 1 - Beam current transformer and peak detected rf envelope.

Initially, the rf frequency is generated by a programmed oscillator and one switches over to the beam control system during the ramp up to the final voltage. Optimum adjustment of the bunching is sensitive to 2-3 parts in  $10^4$  change in the starting frequency, but much less sensitive to the initial value of  $f_{rf}$ . However, best results are obtained with the latter adjusted for 0.67-0.75, the 33 Kc/msec rate required for a moving bucket with  $\Delta R = 0$ . When beam control is initiated, the  $f_{rf}$  dips to near zero briefly ( $\approx 100$   $\mu$ sec) before attaining the nominal synchronous value. The results of this capture process are bunches of up to  $270^\circ$  long and a bucket filling factor of  $N > 0.95$ .

If we define a bunching factor  $B$  given by the ratio of the average to the peak particle density, then a  $B \geq 0.53$  is observed near injection and a  $B \approx 0.5$  is obtained at  $1.19 \times$  injection momentum as shown

\*Work performed under the auspices of the U.S. Department of Energy.

in Fig. 2. Assuming a uniform distribution in longitudinal phase space, the value of  $B$  for these two momenta were calculated and found to agree with the measurements. Using this distribution then, the rms value of the bunch momentum spread was calculated to be 0.487 times the half width. The latter value is 2.28 MeV near injection corresponding to a  $\Delta p/p = 7.13 \times 10^{-3}$ . So that at a dispersion maximum of 2.15 m, the synchrotron oscillations would use up  $\pm 1.53$  cm.

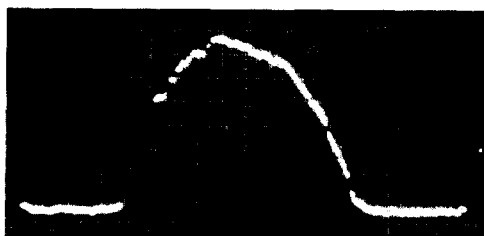


Fig. 2 - Wide-band PUE at 50 nsec/div.

Using the IPM, measurements were made of the circulating beam size without rf voltage applied and with the normal capture program. In the horizontal plane an rms size of 11 mm was obtained without rf voltage and a value of  $\approx 13.5$  mm was measured  $\approx 1.5$  msec from injection with rf voltage, the latter time being after those particles not captured were lost on the vacuum chamber. If we add the rms beam size at the IPM due to momentum spread (6.46 mm) in quadrature with the spiraling beam value of 11 mm, the resulting rms value is 12.75 mm. Operationally, horizontal rms values of 14.5 mm near injection are observed. At a  $\beta_{avg}$  in the AGS (where  $X_p \sim \sqrt{\beta}$ ) the  $3\sigma_x$  beam size would then be 4.2 cm while the available half aperture is 6 cm. However,  $\pm 1$  cm of aperture is used to avoid remnant field effects from fixed extraction magnets. Still, there is potentially space available for larger bunches and studies are being carried out with final voltages in excess of 320 kV.

In order to minimize the voltage induced on the 40 rf cavities by the beam, a fast compensation loop is employed. The signal from a phase pickup is filtered, delayed, amplified, and then added to the normal low level rf output after the AGC stage.<sup>3,4</sup> In this manner a current opposite in phase to the beam current is injected into the cavities. The peak detected rf envelope is shown in Fig. 1, where the slight dip before the rise to the final voltage is a result of adjustments in the compensation circuit. The latter is utilized both at injection and at the end of the acceleration cycle to facilitate debunching of the beam prior to slow extraction. With the relatively large voltages now used for rf capture, the compensation loop is necessary only for intensities  $> 10^{13}$ /pulse but there it is essential.

The longitudinal bunch area with  $V_{rf} = 300$  kV is 1.08 eV sec. This is 1.8 times larger than the 0.6 eV sec value obtained with  $H^+$  injection where a quasi-adiabatic capture process using  $\approx 150$  kV final voltage was employed. Since the strength of the instability encountered in passing the transition energy is  $\sim N_b/A_b^{3/2}$  where  $N_b$  is the number of particles per bunch and  $A_b$  the bunch area, the longitudinal blowup and resulting beam loss should not be

any greater at  $2 \times 10^{13}$  than it was at  $10^{13}$  and  $H^+$  injection. At present with  $1.7 \times 10^{13}$  accelerated, the transition loss can be kept to  $< 10^{12}$  particles by programming a rapid outward radius jump of  $\approx 1.5$  cm (at  $\beta_{avg}$ ) at the transition energy. This speeds up the passage through the transition energy since the latter varies across the AGS aperture.<sup>5</sup> Eventually a  $\gamma_{tr}$  jump system will be installed in the AGS in order to eliminate these losses.

#### Space Charge Effects and Stopband Corrections

The AGS tune space is shown in Fig. 3. A and B are two zero intensity injection operating points at which accelerated beams of  $1.7 \times 10^{13}$  protons/pulse have been achieved. In order to estimate the space charge detuning of a synchronous particle, we use the expression<sup>6</sup>  $\Delta Q_{sc} = N \bar{\beta}_p GF [\pi B b(a+b) (\beta^2 \gamma^3)]^{-1}$  where  $N$  = number of protons,  $\bar{\beta}_p = 1.535 \times 10^{-18}$  M,  $\beta = R/Q$ ,  $a$  and  $b$  are the horizontal and vertical beam half widths and  $G$  is a form factor that depends upon the transverse density distribution.<sup>7</sup> For  $2.2 \times 10^{13}$  protons near injection where  $\beta^2 \gamma^3 = 0.572$  and the bunching factor is  $\approx 0.5$  the 98% emittance beam size as measured with the IPM is  $a \approx 4.2$  cm  $b \approx 2.85$  cm.  $F_v$  is calculated to be 1.31,  $F_H$  0.54 and using  $G = 1.56$  for a Gaussian profile in real space<sup>7</sup> we obtain  $\Delta Q_{ysc} = -0.58$ ,  $\Delta Q_{xsc} = -0.16$ . This is the lowest point of the region in Fig. 3 bounded by A and the solid lines. About 35 msec from injection the beam has  $\approx 450$  MeV of kinetic energy ( $\beta^2 \gamma^3 = 1.75$ ) and points A and B have moved to D and C. Here the beam size at  $1.8 \times 10^{13}$  protons/pulse is  $a \approx 3.27$  cm and  $b = 2.3$  cm and we calculate  $\Delta Q_{ysc} = -0.285$ ,  $\Delta Q_{xsc} = -0.089$ . The solid lines starting at point C extend to meet this point. An estimate of the nonlinear part of the tune shift has been included in drawing the regions bounded by the solid lines<sup>8</sup> shown in the figure. A calculation of the tune shifts at injection using a computer program<sup>9</sup> and a slightly larger beam size give comparable values.

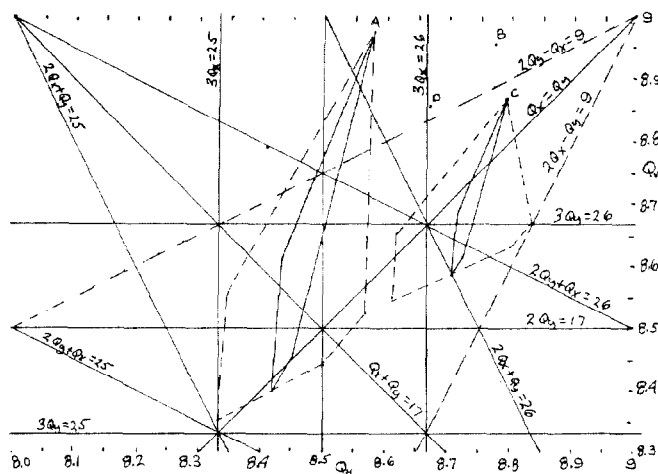


Fig. 3 - AGS tune space.

When we include the tune variations due to chromaticity effects one obtains the regions bounded by the dotted lines. Since the variation of space charge tune shift across the beam was not estimated,

their size represents an upper limit. If the negative horizontal and vertical chromaticities were significantly reduced, the resistive wall instabilities, present at low energies in the AGS, would be too strong to control with the narrow band feedback systems now employed.

IPM measurements (Fig. 4 and 5) show that the normalized horizontal emittance remains constant during the early part of the acceleration cycle. The vertical emittance grows by at most 10% by the time 450 MeV kinetic energy is reached. This is true for both operating lines, i.e. A-D or B-C. For the latter case, all beam losses occur by this time while for the former, the loss rate after capture is lower but usually lasts until 600 MeV kinetic energy is reached.

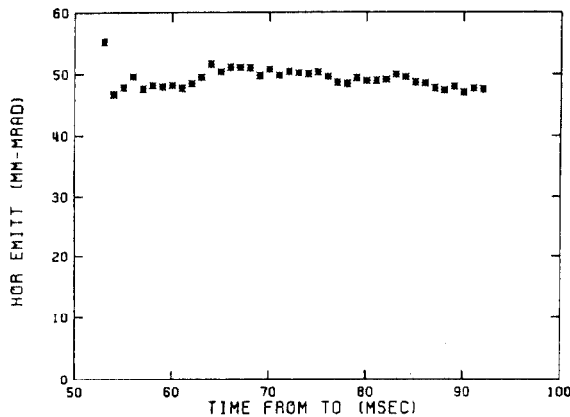


Fig. 4 - Early horizontal emittance from IPM.

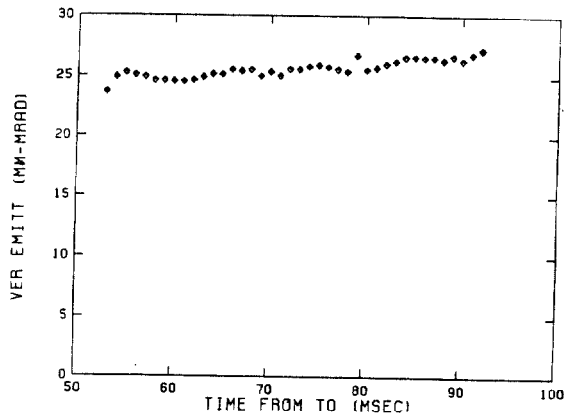


Fig. 5 - Early vertical emittance from IPM.

During injection, capture, and acceleration, many second and third order resonances are crossed repeatedly by the beam. Independent orthogonal correction of the  $2Q_x = 17$  and  $2Q_y = 17$  lines without introducing a  $9^\theta$  or DC component is achievable using 16 of the 24 superperiod symmetric iron core quadrupoles designed for high energy tune controls. Independent orthogonal correction of the  $3Q_x = 26$  and  $2Q_y + Q_x = 26$  lines without a  $17^\theta$  or d.c. component is available using 16 iron core sextupoles. The linear coupling ( $Q_x = Q_y$ ) is compensated by d.c.

currents in 24 air core superperiod symmetric coils. Eight of these are excited to correct the  $Q_x + Q_y = 17$  line without producing a  $9^\theta$  or d.c. component. All the above elements can be excited individually or collectively as indicated. In addition, four air core skew sextupoles are available to correct the  $2Q_x + Q_y = 26$  and  $3Q_y = 26$  lines.

At present, only d.c. excitation is available for the correction element currents. Initial tuning is done using independent orthogonal excitation to obtain a high intensity beam. Individual adjustment of the elements around the currents thus obtained usually produces the maximum intensity. Normally, the closed orbit is corrected with the stopband compensation elements off using a harmonic program. Because the equilibrium orbit does not pass through the center of all these elements they can produce deflections. Since the final intensity is the only criteria used in tuning, a compromise between resonance correction and orbit errors is a likely result of this process.

### Discussion

Successful operation of the AGS across half integral resonances near injection suggest that space charge tune shifts approaching unity can potentially be accommodated. Correction of the 25<sup>th</sup> third-order resonances can be accomplished with the present hardware. In order to get more beam into the machine, continuing studies of the injection process are being carried out. Techniques for filling the horizontal aperture are under investigation and a study of the vertical aperture utilization will be undertaken. Construction and installation of a wide-band transverse feedback system that would permit reduction of the chromaticities is also being considered.

### Acknowledgments

We wish to thank members of the AGS operations staff for their cooperation in this effort and particularly to thank D. Boussard of CERN for his assistance in implementing the beam loading compensation system.

### References

1. D.S. Barton, et al., IEEE Trans. Nucl. Sci., NS-30, 2787 (1983).
2. H. Weisberg, et al., IEEE Trans. Nucl. Sci., NS-30, 2179 (1983).
3. E. Ezura, et al., IEEE Trans. Nucl. Sci., NS-26, 3538 (1979).
4. D. Boussard, CERN SPS/ARF/Int./78-16.
5. F. Pedersen, E. Raka, IEEE Trans Nucl. Sci., NS-26, 3592 (1979).
6. C. Bovet, et al., CERN/MPS-SI/Int. DL/70/4.
7. K.H. Reich, K. Schindl, H. Schonauer, Proc. XII Int. Accel. Conf., Fermilab, 1983, 438-443.
8. J. Gareyte, J.P. Gouber, Proc. 1975 ISABELLE Summer Study, Vol. II, BNL 20550, 411.
9. J. Claus, IEEE Trans. Nucl. Sci., NS-22, No. 3, 1926 (1975).